Available online at www.sciencedirect.com

SCIENCE DIRECT®

Biochimica et Biophysica Acta 1665 (2004) 92–100

BIOCHIMICA ET BIOPHYSICA ACTA

BBA

http://www.elsevier.com/locate/bba

Effect of electric field vectoriality on electrically mediated gene delivery in mammalian cells

Cécile Faurie[1], Emilie Phez[1], Muriel Golzio, Christine Vossen, Jeanne-Claire Lesbordes, Christine Delteil, Justin Teissié, Marie-Pierre Rols*

Institut de Pharmacologie et de Biologie Structurale du CNRS UMR 5089, 205, route de Narbonne, 31077 Toulouse cedex, France

Received 5 March 2004; received in revised form 22 June 2004; accepted 29 June 2004
Available online 26 July 2004

Abstract

Electropermeabilization is a nonviral method used to transfer genes into living cells. Up to now, the mechanism is still to be elucidated. Since cell permeabilization, a prerequired for gene transfection, is triggerred by electric field, its characteristics should depend on its vectorial properties. The present investigation addresses the effect of pulse polarity and orientation on membrane permeabilization and gene delivery by electric pulses applied to cultured mammalian cells. This has been directly observed at the single-cell level by using digitized fluorescence microscopy. While cell permeabilization is only slightly affected by reversing the polarity of the electric pulses or by changing the orientation of pulses, transfection level increases are observed. These last effects are due to an increase in the cell membrane area where DNA interacts. Fluorescently labelled plasmids only interact with the electropermeabilized side of the cell facing the cathode. The plasmid interaction with the electropermeabilized cell surface is stable and is not affected by pulses of reversed polarities. Under such conditions, DNA interacts with the two sites of the cell facing the two electrodes. When changing both the pulse polarity and their direction, DNA interacts with the whole membrane cell surface. This is associated with a huge increase in gene expression. This present study demonstrates the relationship between the DNA/membrane surface interaction and the gene transfer efficiency, and it allows to define the experimental conditions to optimize the yield of transfection of mammalian cells.

Keywords: Electric field; Electroporation; Permeabilization; Gene transfer; Videomicroscopy

1. Introduction

Viral vectors are considered to be the most efficient method for gene transfer, but they are often associated to host inflammatory and immune responses [1]. Nonviral methods of gene delivery have therefore been investigated for years. Among them, a physical method, electropermeabilization, also named electroporation (for review, see Ref. [2]), based on the delivery of electric pulses to cells, has been developed in the early 1980s [3]. Since then, electropermeabilization has been used with increasing popularity for introducing a large variety of molecules into cells [4,5]. For the last 10 years, medical applications of this method have been successfully introduced for enhanced antitumoral drug delivery to patients, a method called electrochemotherapy [6], and for in vivo transfer of genes into the skin, liver, melanoma and skeletal muscle cells, a method called electrogenetherapy [6–11].

Molecular mechanisms are still largely unknown. Formation of aqueous pores was proposed to be the basis of electropermeabilization [12]. Many groups have reported data about the mechanisms of electrically induced permeabilization and gene transfer [13–17]. Indeed, several models have been proposed in the case of mammalian cells where the plasmid crosses the membrane (1) due to the existence of long-lived "electropores" [3,16,17], (2) eventually after a binding step at the cell surface and then diffusion through the "electropores" [16], (3) during

* Corresponding author. Tel.: +33 5 61 17 58 11; fax: +33 5 61 17 59 94.
E-mail address: marie-pierre.rols@ipbs.fr (M.-P. Rols).
[1] The two first authors had the same contribution.

0005-2736/$ - see front matter © 2004 Elsevier B.V. All rights reserved.
doi:10.1016/j.bbamem.2004.06.018

delivery of the electric pulses due to electrophoretic forces associated with the external field [13,18], or (4) by adsorption by sphingosine/DNA interactions, insertion and passage of DNA through a hydrophilic percolated porous zone [14].

Our experimental data led to the conclusion that millisecond electric pulses induced an interaction between the electropermeabilized membrane and the plasmid which is electrophoretically pushed against the cell surface. This allowed the insertion of the plasmid DNA, which crossed the membrane during the minutes following pulsation [19,20]. We recently demonstrated this working model by visualizing at the single-cell level the first steps of DNA transfer induced by electric pulses [20]. Permeabilization occurs at the sides of the cell membrane facing the two electrodes under electrical conditions optimized for gene transfer. At the opposite, DNA molecules only interact with the electropermeabilized side of the cell facing the cathode where they are trapped in microdomains. Thus, although membrane permeabilization occurs at the two sides of the cell, only one side is competent" for gene transfer. Any increase in the "competent" area of the cell membrane where DNA interacts should increase gene transfer and expression level [19].

The aim of the present study was to go further into the description of the mechanism of gene transfer by electric pulses. For this purpose, our strategy consisted on increasing the surface of interaction of the DNA with membrane by changing the pulse polarity and the pulse direction. We therefore investigated their consequences on plasma membrane permeabilization, DNA/membrane interaction and gene expression.

2. Materials and methods

2.1. Cells

Chinese hamster ovary (CHO) cells were used. The WTT clone was selected for its ability to grow in suspension or plated. They were grown in suspension in MEM medium as previously described [21]. Their ability to grow on a support after being maintained in suspension is direct evidence of their viability.

2.2. DNA staining

A 4.7-kb plasmid, pEGFP-C1 (Clonetech, Palo Alto, CA), carrying the gene of the Green Fluorescent Protein under control of the CMV promoter, was stained stoichiometrically with the DNA intercalating thiazole orange homodimer dye TOTO-1 (Molecular Probes, Eugene, OR) during 60 min on ice at a base pair to dye ratio of 5 [22]. Plasmid was prepared from transformed *E. coli* by using Maxiprep DNA purification system according to manufacturer instructions (Qiagen, Chatsworth, CA).

2.3. Electropulsation apparatus

Electropulsation was operated by using a CNRS cell electropulsator (Jouan, St Herblain, France) which delivered square-wave electric pulses. An oscilloscope (Enertec, St. Etienne, France) monitored pulse shapes. A homemade polarity inverter gave inversion of the polarity between each pulse. Electrodes were connected to the voltage generator.

For electropermeabilization and gene transfer, the electropulsation chamber was designed using stainless steel parallel plates electrodes (10-mm length, 10-mm width) brought on contact on plastic coverslip (Thermanox, Nunc). For microscopy observations, the electropulsation chamber was designed using two stainless steel parallel rods (0.5-mm diameter, 10-mm length, 7-mm width) put on a microscope glass coverslip chamber (Labteck II system).

2.4. Electropermeabilization

Cells were cultured on plastic coverslip (13-mm diameter, Thermanox, Nunc) put in 24-well chamber at 10^5 cells per well (i.e., 2 cm^2) 24 h before electropulsation. At the time of the experiment, the coverslip was transferred to a new well. Permeabilization of cells was performed by delivery of long electric pulses required to transfer genes and to load macromolecules into cells [23,24]. Culture medium was removed and replaced by 1-ml pulsing buffer (10 mM phosphate, 1 mM $MgCl_2$, 250 mM sucrose, pH 7.4). Penetration of propidium iodide (100 μM) in pulsing buffer was used to monitor permeabilization. Eight pulses lasting 5 ms at a frequency of 1 Hz were applied at a given electric field intensity at room temperature. Five minutes after pulses delivery, membrane resealing has occurred and cells were trypsinized and analysed by flow cytometry (Becton Dickinson FACScan) to determine both the percentage of permeabilized cells (i.e., the percentage of fluorescent cells) and its efficiency (i.e., the level of fluorescence associated with this permeabilization).

2.5. Electrotransfection

Cells (10^5) were grown on 13-mm plastic coverslip (Thermanox, Nunc, Polylabo). pEGFP-C1 plasmid containing pulsing buffer was used. For each condition, 4 μg of plasmid was used. Eight pulses lasting 5 ms at a frequency of 1 Hz were applied at a given electric field intensity at room temperature. Then, cells were incubated for 10 min at 30 °C. They were cultured in 24-well chambers with 1.5 ml of culture medium for 24 h at 37 °C in a 5% CO_2 incubator. Only plated cells (i.e., viable cells) were taken into account in the assay. Cells were harvested by trypsinization and analysed by flow cytometry to evaluate both the percentage of transfection (i.e.,

percentage of GFP-expressing cells) and the gene expression (i.e., mean level of fluorescence associated with this transfection).

2.6. Cell viability

Cell viability was determined by the ability of cells to grow and divide over a 24-h period as previously described. Cells were pulsed, kept for 10 min at 30 °C and then grown in Petri dishes after adding 1 ml of culture medium for 24 h at 37 °C in a 5% CO_2 incubator. Viability was measured by monitoring cells growth through a coloration method [25].

2.7. Microscopy

Cells were seeded in Labteck II chambered coverglass system (Nunc, Naperville, Il) 30 min before the experiment in order to keep them spherical but attached to the support. The chamber was placed on the stage of an inverted digitized microscope (Leica DMIRB, Wetzlar, Germany). Cells were observed with a Leica 100×, 1.3 NA oil immersion objective. The wavelengths were selected by using the Leica L4 filter block for the TOTO-1 labeled DNA and the Leica M2 filter block for the PI labelled cells. Images were recorded with the CELLscan System from Scanalytics (Billerica, MA) equipped with a Photometrics cooled CCD camera (12-bit grey levels) (Princeton Instrument, Inc.). Analysis of gene transfer and profiles of intensity were obtained by fluorescence microscopy imaging using cellview software.

3. Results

We compared the effect of four different trains of 8 rectangular electrical pulses lasting 5 ms delivered in intervals of 1 s and sketched in Fig. 1: (i) a train of 8 unipolar pulses (normal condition, Fig. 1A), (ii) a train of 8 oppositely oriented pulses (inverted condition, Fig. 1B), (iii) a train of 4 unipolar pulses followed by a train of 4 unipolar pulses applied after rotation of the electrodes of 90° (crossed condition, Fig. 1C), and (iv) a train of 4 oppositely oriented pulses followed by a train of 4 oppositely oriented pulses applied after rotation of the electrodes of 90° (crossed-inverted condition, Fig. 1D). Adherent cells were used in order to avoid any artefact due to cell rotation during pulses delivery.

3.1. Cell permeabilization under electrotransfection conditions

Under such electric pulse conditions, cell viability was affected by increasing electric field intensity, but with no significant difference between each condition (data not shown).

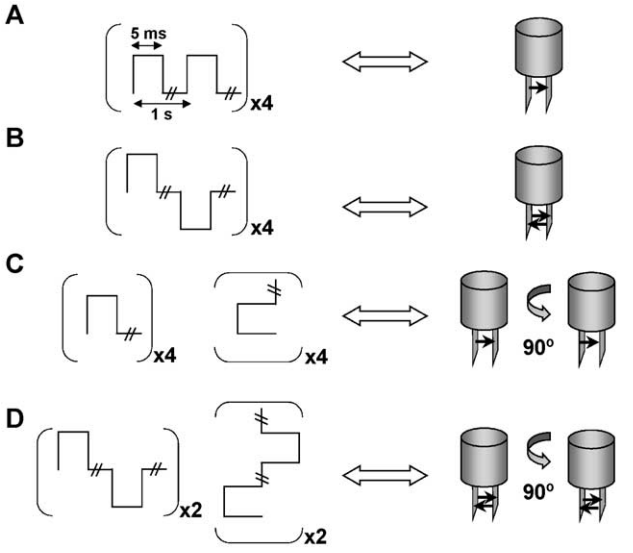

Fig. 1. Schema of the 4-pulse sequences defined as Normal, Crossed, Inverted and Crossed-Inverted conditions. Eight pulses lasting 5 ms at a frequency of 1 Hz were applied for different values of electric field. (A) Normal condition (a train of 8 unipolar pulses), (B) Inverted condition (a train of 8 oppositely oriented pulses), (C) Crossed condition (a train of 4 unipolar pulses followed by 90° rotation by a train of 4 unipolar pulses) and (D) Crossed-Inverted condition (a train of 4 oppositely oriented pulses followed by a train of 4 oppositely oriented pulses).

Permeabilization was quantified by monitoring the penetration of PI into cells. Eight pulses lasting 5 ms were then applied under 4-pulse sequences corresponding to normal, inverted, crossed, and crossed-inverted conditions. Due to the difference in geometry between electrodes (square area) and plastic coverslip (circle area), only 80% of the cellular population on the coverslip were submitted to electric pulses. As shown in Fig. 2A, up to 80% of the cells were permeabilized under normal conditions whatever the electric field intensity when above 0.4 kV/cm. This percentage was not statistically affected by changing the polarity and orientation of the electric pulses in terms of percentage but the highest increase in amount of dye uptake was observed for crossed-inverted condition (Fig. 2B).

3.2. Visualization of permeabilization

The direct visualization of permeabilization was performed at the single-cell level within the seconds following delivery of electric pulses [20]. Permeabilization was observed at the sides of the cell membrane facing the two electrodes as shown by PI entrance into cytoplasm (Fig. 3A,B,E and F). Ten seconds after the pulsation PI had diffused across the cytoplasm. In all conditions, less than 1 min after electrical pulses, staining of the nucleus of the permeabilized cells by PI was observed (data not shown). The observation of early events in crossed condition was therefore prohibited due to technical time necessary for electrode rotation.

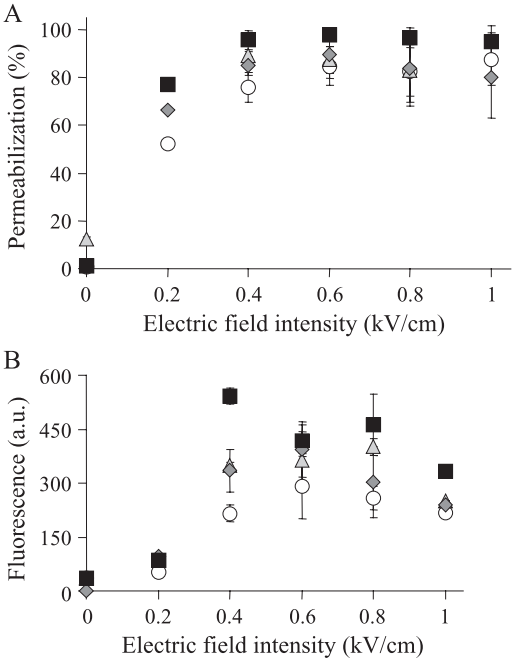

Fig. 2. Effect of electric field intensity and vectoriality on CHO cell permeabilization. (A) Percentage of permeabilized cells. (B) Fluorescence intensity associated with the permeabilization. Eight pulses of 5-ms duration, 1 Hz, were applied to plated cells in pulsing buffer for the 4-pulse sequences: Normal (○), Crossed (▲), Inverted (◆), Crossed-Inverted (■). Permeabilization was quantified by propidium iodide entrance by flow cytometry.

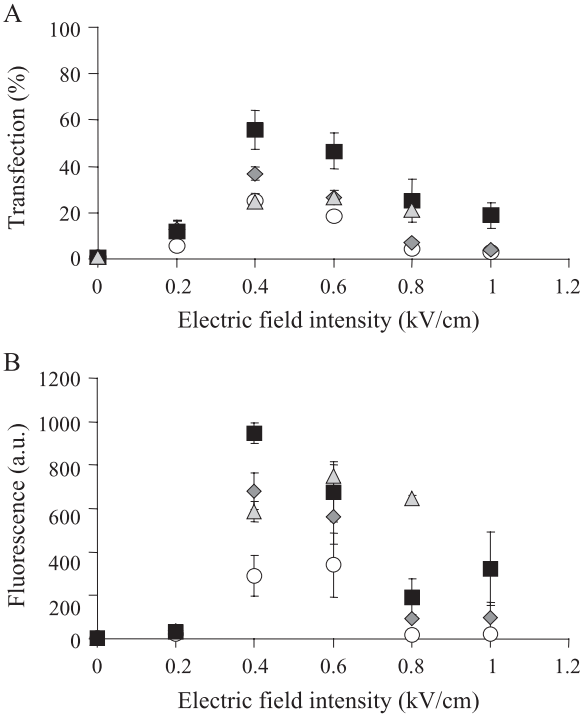

Fig. 4. Effect of electric field intensity and vectoriality on CHO cell gene expression. (A) Percentage of electrotransfected cells. (B) Associated mean fluorescence level of GFP expressing cells. Eight pulses of 5-ms duration, 1 Hz, were applied to plated cells in pulsing buffer for the 4-pulse sequences: Normal (○), Crossed (▲), Inverted (◆), Crossed-Inverted (■). GFP expression was detected 24 h after electric treatment by flow cytometry.

Under normal condition, the fluorescence intensity profile showed that the fluorescence associated with the permeabilized site facing the anode was always higher than the fluorescence intensity facing the cathode (Fig. 3C and D). This asymmetric permeabilization at the two sites of cell membrane facing the electrodes was no more observed when pulse polarity was changed. In that case, permeabilization was symmetric (Fig. 3G and H).

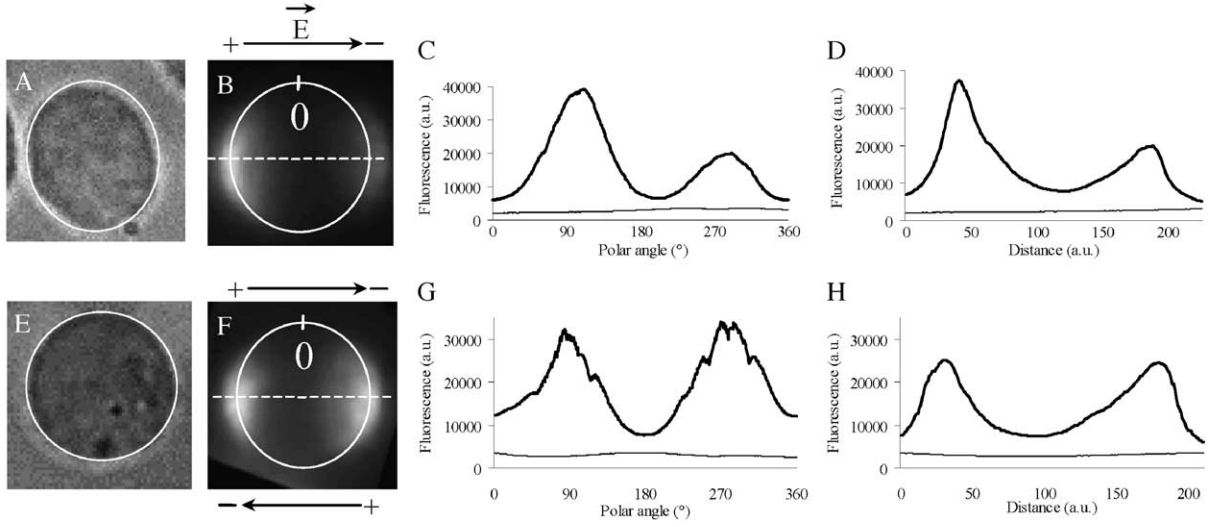

Fig. 3. Fluorescence profiles of permeabilized areas. Cells were incubated in the presence of 100 μM of propidium iodide in the pulsing buffer. Eight pulses of 5-ms duration, 1 Hz, at 0.8 kV/cm were applied to cells for the 2-pulse sequences: Normal (A, B), Inverted (E, F). Light contrast images before pulsation (A, E). Fluorescence images 1 s after pulsation (B, F). The time exposure of the camera was set at 0.1 s. Fluorescence intensity profile along the cell membrane highlighted by the white line (B, F). Fluorescence intensity radial profile along dotted lines (B, F). Thin lines represent the fluorescence detected before pulse delivery (C, D, G, H). Thick lines represent the fluorescence intensity 1 s after electropulsation (C, D, G, H). The black arrow on the top of the figure indicates the direction of the electric field (B, D). (a.u., arbitrary units).

3.3. Cell electrotransfection

Transfection was quantified by GFP expression 24 h after cell electropulsation. No transfected cell was detected in the absence of electric pulses or in the absence of DNA. For the four conditions, electrotransfection was only detected for electric field values leading to permeabilization (Fig. 4A and B). Transfection threshold values were equal to 0.2 kV/cm, as obtained for cell permeabilization.

Transfection percentage up to 20% was obtained under normal conditions; this percentage decreased by increasing electric field intensities above 0.6 kV/cm, a phenomenon associated to a marked loss in cell viability. For optimal electric field intensity (0.4 kV/cm), no change in transfection percentage was noticed in crossed condition. Inverted condition led to a significant increase in transfection: up to 40% of cells expressed the reporter gene. Under crossed-inverted electric pulse condition, the percentage of transfected cells reached 60% (Fig. 4A).

These increases in transfection percentage were correlated with gene expression. Taking normal condition as reference, a twofold increase in inverted and crossed conditions was observed, while a three-time increase in fluorescence was observed for crossed-inverted condition (Fig. 4B).

3.4. Videomicroscopy analysis of DNA/membrane interaction

Direct visualization of DNA interaction with membrane, i.e., of the first step of gene transfer, was performed at the single-cell level by using fluorescent labelled plasmid DNA. Cells immersed in the labelled DNA in solution appeared in black (data not shown). No fluorescence due to spontaneous adsorption of DNA to the plasma membrane was detected as already described [20]. When electric pulses higher than the values required to permeabilize cells were applied, spots appeared at the membrane level, and were strictly only present on the side of the cell facing the cathode (Fig. 5A and B). This vectoriality in DNA/membrane interaction was one of the main differences with entrance of small-sized molecules, which took place on the sides of the cell facing the two electrodes, and mainly at the anode facing one. Under inverted condition, a symmetrical fluorescence

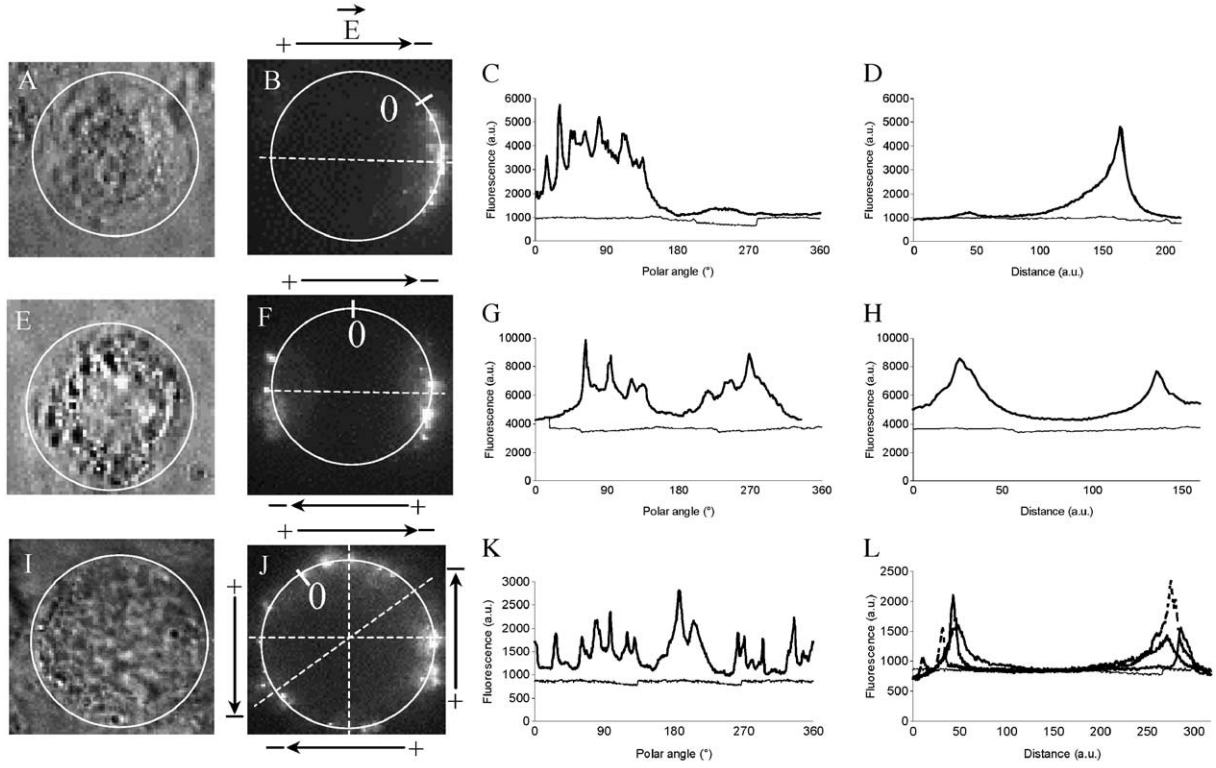

Fig. 5. Fluorescence microscopy observation of the DNA-membrane interaction areas. Cells were incubated in the presence of TOTO-1-labelled DNA (pEGFP-C1) in the pulsing buffer. Eight pulses of 5-ms duration, 1 Hz, at 0.6 kV/cm were applied to plated cells for three pulses sequences: Normal (A, B), Inverted (E, F), Crossed-Inverted (I, J). The time exposure of the camera was set at 1 s. Light contrast image before pulsation (A, E, I). Fluorescence images 30 s after the pulsation (B, F, J). Labelled DNA interacted with permeabilized area of the membrane facing the cathode. The black arrow on the figure indicates the direction of the electric field. Fluorescence intensity profiles at the membrane level associated. Fluorescence intensity profiles (C, G, K) are analysed along the cell membrane highlighted by the white lines in B, F, J, respectively. Fluorescence intensity radial profiles (D, H, L) are analysed along dotted lines in B, F, J, respectively. Thin lines represent the fluorescence detected before pulse delivery. Thick lines represent the fluorescence intensity after electropulsation. (a.u., arbitrary units).

increase was observed on both sides of the cell facing the electrodes (Fig. 5E and F). Moreover, under crossed-inverted condition, DNA was observed all around the permeabilized cell membrane (Fig. 5I and J). Whatever the conditions, DNA always appeared as spots at the membrane.

In Fig. 5 (C, D, G, H, K and L), fluorescence intensity profiles were measured at the cell membrane level before and after electric pulse delivery. Before electropulsation, the basal fluorescence level was the same all around the membrane (full line). One second after electropulsation, fluorescence sharply increased. The quantitative analysis showed that fluorescence was clearly not homogeneous but present as "spots" for all conditions. These DNA-interacting zones were present in front of the cathode under normal electric pulses delivery (Fig. 5C and D), facing the two-electrode sites when pulse polarity was changed (Fig. 5G and H) and all around the cell when change of pulses direction was combined with inversion of pulse polarity (Fig. 5K and L).

4. Discussion

The aim of the present work was to study the relationship between electrically mediated membrane permeabilization and gene transfer. Our hypothesis was that any increase in permeabilized membrane area should increase gene expression. Experimental evidence has been obtained by increasing the electric field strength. This was first observed on cell population [19] and then confirmed by a direct visualization of the phenomenon at the single cell level [20]. However, in this approach, the DNA electrophoretic drag was concomitantly affected, as it was directly proportional to electric field strength. Our new strategy consisted on using electric pulse conditions leading DNA to interact with different sites of the electropermeabilized plasma membrane with no difference in the number and strength of electric field. For this purpose, pulses with different polarity and direction were applied at given electric field intensities. Consequences were then analyzed both at the single-cell and population levels in order to, respectively, get access to the first steps in gene transfer, i.e., DNA/membrane interaction, and to the long-term one, i.e., gene expression.

The transmembrane potential difference U is the sum between the resting value of cell membrane U_o and the electroinduced value U_M.

$$U_M = -\Delta\varphi_{(M)} = fg(\lambda)rE\cos\theta \quad (1)$$

in which f is a shape factor, $g(\lambda)$ designates a complex function of the specific conductivities of the membrane, the pulsing buffer and the cytoplasm, r is the radius of the cell, E the field intensity and θ the angle between the direction of the field and the normal to the membrane at point M on the cell surface.

For mammalian cells, the resting potential of the cell membrane is negative with respect to the cell exterior. Consequently, when the field is applied, values of the resulting transmembrane potential are higher at the pole facing the positive electrode than at the pole facing the negative one. This results in the asymmetry of electropermeabilization [26–29]. Under unipolar conditions (Fig. 3B), permeabilization was actually detected at the cell membrane sides facing the two electrodes, the permeabilized membrane area facing the anode being always higher than the one facing the cathode. Bipolar pulses counterbalanced this asymmetry and increased the permeabilized membrane area (Fig. 3F). Visualisation of permeabilization in crossed and crossed-inverted conditions was not technically possible. Permeabilized membrane areas in these conditions are cartooned in Fig. 6.

Eq. (1) predicts that cell permeabilization by electric pulses is not only a function of electric field intensity and cell size but also of cell shape and orientation. This has to be taken into account when working with adherent ellipsoidal cells. Any change in these parameters should be associated with changes in permeabilization. Previous mathematical simulations have calculated both numerically and analytically the induced transmembrane potential for different cell orientations. This potential decreased from its maximum value, when the longest axis of the cell was parallel to the electric field, to its minimum value when the longest axis of the cell was perpendicular to the electric field [30–32]. In our work, we analyzed experimentally the effects on a cell population with a random orientation distribution. Consequently, the pulse strength required to permeabilize 80% of cells (EC80) appeared unchanged according to pulse polarity and direction (Fig. 2A). Kotnik et al. [33,34] showed that pulse strengths were lowered when using bipolar short pulses. Under our conditions, longer pulses were used, bringing a sharp increase in the percentage of permeabilized cells above 0.2 kV/cm. Otherwise, above 0.4 kV/cm, the percentage of permeabilized cells was not statistically affected by changing pulse polarity and ori-

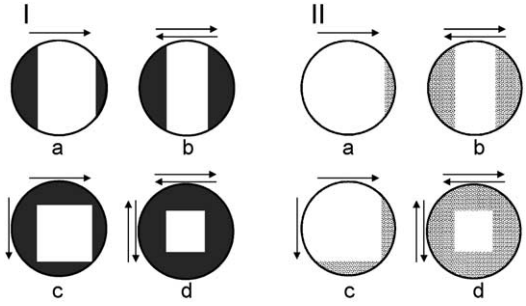

Fig. 6. Model of mammalian cell competent areas for permeabilization and gene transfer. Cartoon of the permeabilized membrane area (I) and the DNA/membrane interaction region (II) according to the four-pulse sequences: normal condition (a), inverted condition (b), crossed condition (c), crossed-inverted condition (d). Black areas indicate regions where permeabilization occurred. Dotted areas indicate region where DNA interacted with permeabilized membrane.

entation (Fig. 2A). As under normal conditions, it reached its maximal value, any possible positive effects of changes in pulse polarity and direction should not have been detected. A significant 50% increase in the amount of dye uptake was observed for inverted and crossed conditions while it reached 150% for crossed-inverted conditions, both with respect to normal conditions (Fig. 2B).

Square-waved pulses led to a homogeneous long-lived and local permeabilization. Dye inflow, Φ, occurred mostly after the pulses driven by the transmembrane concentration gradient and was therefore proportional to the permeabilized area. In the case of a sphere, it was proportional to:

$$\Phi = k\mathrm{At}(1 - \mathrm{Es}/E) \quad (2)$$

in which k is a constant depending on E, At the total cell surface, Es the threshold value below which no permeabilization occurs [35]. Increasing the permeabilized membrane area increased the exchange of small molecules across the membrane [28,35]. In the present study, permeabilization as well as transfection experiments were done on adherent CHO cells, i.e., ellipsoidal cells with a random orientation. According to previous results [32], we have calculated and compared permeabilized membrane areas of ellipsoidal and spherical cells (Table 1). The conclusion is that electric pulses permeabilized the same membrane area of ellipsoidal and spherical cells. We have done further calculations on spherical cells. Modifying pulse polarity and direction increases the permeabilized membrane area and thus should bring an increase in dye influx as observed. Relationship between electric field intensity and the cap angle θ_p of the cell membrane permeabilized area is:

$$|\cos\theta| = \mathrm{Es}/E \quad (3)$$

with Es less than 0.2 kV/cm and θ larger than 45°; E is above 0.28 kV/cm. So in all conditions tested (E>0.3 kV/cm), there is an overlap and not a strict additivity between permeabilized areas triggered in crossed and crossed-inverted conditions (Fig. 6). Consequently, the permeabilized membrane area and, as such, permeabilization efficiency were less than two times higher in crossed conditions and less than four times higher in crossed-inverted conditions than in normal ones as observed.

While, under unipolar electric pulses, permeabilization was observed on both cell sides, DNA/membrane interacting zones were only present in front of the cathode (Fig. 5B). This confirms previous results showing that DNA interacts only with the electropermeabilized membrane area facing the negative electrode [20]. When pulse polarity was changed, DNA molecules interacted in the zones facing the two electrodes (Fig. 5F). Interaction was observed all around the cell when change of pulses direction was combined with inversion of pulse polarity (Fig. 5J). These results actually show that increasing the permeabilized membrane area, mainly by changing pulses direction, and the DNA interacting zones, by changing pulse polarity, led to a sharp increase in DNA/membrane interaction (Fig. 6).

At optimal electric field intensity, i.e., 0.4 kV/cm, 20% of cells were transfected by unipolar pulses. No change in transfection percentage was noticed in crossed condition. Inverted condition led to a significant increase in transfection, up to 40% of cells expressing the reporter gene. Under crossed-inverted electric pulse condition, the percentage of transfected cells reached 60% (Fig. 4A). This increase in transfection percentage was correlated with an increase in gene expression. Taking normal condition as reference, a two-time increase in inverted and crossed conditions was observed, while a three-time increase in fluorescence was observed for crossed-inverted condition (Fig. 4B). In our previous study, increase in transfection obtained by increasing field intensities was linearly related to the extent of permeabilized cell surface, as long as the viability of the cell population was not strongly affected [19]. Changing pulse polarity and orientation increases permeabilized membrane area and DNA/membrane interacting zones, and, consequently, can explain the increase in gene expression (Fig. 6).

By using 60-kHz square-waved train pulses, an increase in gene expression was observed by changing the pulse polarity [36]. DNA electrophoresis was reported to have a key role for DNA transfer [18,37]. Increasing electric field intensity had a contribution both on the permeabilized membrane area and on the electrophoretic migration of the plasmid towards the permeabilized membrane [19]. In our study, performed at given electric field strengths and duration, DNA, brought in contact to the cell surface resulting from electrophoretic migration, should be unchanged by pulse polarity and direction. Increasing pulse number has been reported to increase gene expression up to a plateau value [23]. An eventual saturating effect in unipolar conditions by applying 8 pulses could therefore

Table 1
Comparison between the percentages of permeabilized cell area of ellipsoidal and spherical cells for different electric field intensities

Electric field (V/cm)	300	350	400	450	500	550	600
Δϕc (α=0°) (%)	12	23	30	38	45	48	53
Δϕc (α=90°) (%)	0	4	13	26	34	41	47
Δϕc mean (%)	6	13.5	21.5	32	39.5	44.5	50
Δϕs (%)	0	14	25	33	40	45	50

Δϕc: cell area above the critical transmembrane potential for electropermeabilization for a prolate spheroid with ρ=10/5 (corresponding to ellipsoidal cells), a resting transmembrane potential Δϕo=−50 mV (from Valic et al., [32]).
α=0°: angle of orientation between the symmetry axis of the spheroid and the external electric field.
α=90°: angle of orientation between the symmetry axis of the spheroid and the external electric field.
Δϕc mean: average between Δϕc (α=0°) and Δϕc (α=90°).
Δϕs: cell area above the critical transmembrane potential for electropermeabilization for a spherical cell. With Δϕs=1−Es/E, threshold of permeabilization Es=0.2 kV/cm (from Valic et al. [32]).

explain the positive effects of the modification of pulse polarity and orientation on gene expression.

In conclusion, our results obtained both at the single-cell and population levels support our conclusions that there is a fair agreement between the increase in permeabilized membrane area and the improvement in permeabilization and gene expression. Clearly, a multidirectional electropulsation protocol should provide a great advantage for membrane permeabilization and gene transfer. This has successfully been used for electrofusion experiments where contact between permeabilized areas is a critical factor for fusion and yield [38], and in electrochemotherapy to compensate in vivo electric field inhomogeneity and non-spherical cells shape deviations [39]. It should be of great interest for in vivo gene transfer where the efficiency is always lower than in in vitro experiment. Interstitial transport of DNA is a crucial step in gene therapy due to contacts between cells [40]. One may propose that inverted or changing the orientation of the pulses could increase gene transfer and therefore expression by the increase of plasmid DNA diffusion in the tissue. This has been indeed recently applied in muscles [41,42].

Acknowledgements

The authors wish to thank Claire Millot for her help in cell culture and Dr. Stéphane Orlowski for helpful discussion and rereading of the manuscript. The Association Française contre les Myopathies (AFM), the Fondation pour la Recherche Médicale (FRM) and the European Union Project «Cliniporator» have supported this work.

References

[1] A.E. Trezise, In vivo DNA electrotransfer, DNA Cell Biol. 21 (2002) 869–877.
[2] T.Y. Tsong, Electroporation of cell membranes, Biophys. J. 60 (1991) 297–306.
[3] E. Neumann, M. Schaefer-Ridder, Y. Wang, P.H. Hofschneider, Gene transfer into mouse lyoma cells by electroporation in high electric fields, EMBO J. 1 (1982) 841–845.
[4] H. Potter, Application of electroporation in recombinant DNA technology, Methods Enzymol. 217 (1993) 461–478.
[5] S. Orlowski, L.M. Mir, Cell electropermeabilization: a new tool for biochemical and pharmacological studies, Biochim. Biophys. Acta 1154 (1993) 51–63.
[6] L.M. Mir, L.F. Glass, G. Sersa, J. Teissie, C. Domenge, D. Miklavcic, M.J. Jaroszeski, S. Orlowski, D.S. Reintgen, Z. Rudolf, M. Belehradek, R. Gilbert, M.P. Rols, J. Belehradek Jr., J.M. Bachaud, R. DeConti, B. Stabuc, M. Cemazar, P. Coninx, R. Heller, Effective treatment of cutaneous and subcutaneous malignant tumours by electrochemotherapy, Br. J. Cancer 77 (1998) 2336–2342.
[7] A. Titomirov, S. Sukharev, E. Kistanova, In vivo electroporation and stable transformation of skin cells of newborn mice by plasmid DNA, Biochim. Biophys. Acta 1088 (1991) 131–134.
[8] R. Heller, M. Jaroszeski, A. Atkin, D. Moradpour, R. Gilbert, J. Wands, C. Nicolau, In vivo gene electroinjection and expression in rat liver, FEBS Lett. 389 (1996) 225–228.
[9] M.P. Rols, C. Delteil, M. Golzio, P. Dumond, S. Cros, J. Teissie, In vivo electrically mediated protein and gene transfer in murine melanoma, Nat. Biotechnol. 16 (1998) 168–171.
[10] H. Aihara, J.-I. Miyazaki, Gene transfer into muscle by electroporation in vivo, Nat. Biotechnol. 16 (1998) 867–870.
[11] T. Muramatsu, A. Nakamura, H.M. Park, In vivo electroporation: a powerful and convenient means of nonviral gene transfer to tissues of living animals, Int. J. Mol. Med. 1 (1998) 55–62.
[12] J.C. Weaver, Electroporation: a general phenomenon for manipulating cells and tissues, J. Cell Biochem. 51 (1993) 426–435.
[13] V. Klenchin, Electrotransfection of cells: properties and possible mechanisms, Biol. Membr. 7 (1994) 1–16.
[14] N.I. Hristova, I. Tsoneva, E. Neumann, Sphingosine-mediated electroporative DNA transfer through lipid bilayers, FEBS Lett. 415 (1997) 81–86.
[15] T. Xie, L. Sun, H. Zhao, J. Fuchs, T. Tsong, Study of mechanisms of electric field-induced DNA transfection: IV. Effects of DNA topology on cell uptake and transfection efficiency, Biophys. J. 63 (1992) 1026–1031.
[16] T. Xie, T. Tsong, Study of mechanisms of electric field-induced DNA transfection: V. Effects of DNA topology on surface binding, cell uptake, expression, and integration into host chromosomes of DNA in the mammalian cell, Biophys. J. 65 (1993) 1684–1689.
[17] P.G. de Gennes, Passive entry of a DNA molecule into a small pore, Proc. Natl. Acad. Sci. U. S. A. 96 (1999) 7262–7264.
[18] S.I. Sukharev, V.A. Klenchin, S.M. Serov, L.V. Chernomordik, A. Chizmadzhev Yu, Electroporation and electrophoretic DNA transfer into cells. The effect of DNA interaction with electropores, Biophys. J. 63 (1992) 1320–1327.
[19] H. Wolf, M.P. Rols, E. Boldt, E. Neumann, J. Teissie, Control by pulse parameters of electric field-mediated gene transfer in mammalian cells, Biophys. J. 66 (1994) 524–531.
[20] M. Golzio, J. Teissie, M.P. Rols, Direct visualization at the single-cell level of electrically mediated gene delivery, Proc. Natl. Acad. Sci. U. S. A. 99 (2002) 1292–1297.
[21] M.P. Rols, P. Femenia, J. Teissie, Long-lived macropinocytosis takes place in electropermeabilized mammalian cells, Biochem. Biophys. Res. Commun. 208 (1995) 26–35.
[22] H. Rye, S. Yue, D. Wemmer, M. Quesada, R. Haugland, R. Mathies, A. Glazer, Stable fluorescent complexes of double-stranded DNA with bis-intercalating asymmetric cyanine dyes: properties and applications, Nucleic Acids Res. 20 (1992) 1803–1812.
[23] M.P. Rols, D. Coulet, J. Teissie, Highly efficient transfection of mammalian cells by electric field pulses. Application to large volumes of cell culture by using a flow system, Eur. J. Biochem. 206 (1992) 115–121.
[24] S. Hui, Effects of pulse length and strength on electroporation efficiency, Methods Mol. Biol. 55 (1995) 29–40.
[25] B. Gabriel, J. Teissie, Spatial compartmentation and time resolution of photooxidation of a cell membrane probe in electropermeabilized Chinese hamster ovary cells, Eur. J. Biochem. 228 (1995) 708–710.
[26] E. Tekle, R.D. Astumian, P.B. Chock, Electro-permeabilization of cell membranes: effect of the resting membrane potential, Biochem. Biophys. Res. Commun. 172 (1990) 282–287.
[27] M. Hibino, H. Itoh, K. Kinosita Jr., Time courses of cell electroporation as revealed by submicrosecond imaging of transmembrane potential, Biophys. J. 64 (1993) 1789–1800.
[28] B. Gabriel, J. Teissie, Direct observation in the millisecond time range of fluorescent molecule asymmetrical interaction with the electropermeabilized cell membrane, Biophys. J. 73 (1997) 2630–2637.
[29] B. Gabriel, J. Teissie, Time courses of mammalian cell electropermeabilization observed by millisecond imaging of membrane property changes during the pulse, Biophys. J. 76 (1999) 2158–2165.
[30] T. Kotnik, D. Miklavcic, Analytical description of transmembrane voltage induced by electric fields on spheroidal cells, Biophys. J. 79 (2000) 670–679 [erratum appears in Biophys. J. 2003 Mar; 84(3):2130.].

[31] J. Gimsa, D. Wachner, Analytical description of the transmembrane voltage induced on arbitrarily oriented ellipsoidal and cylindrical cells, Biophys. J. 81 (2001) 1888–1896.
[32] B. Valic, M. Golzio, M. Pavlin, A. Schatz, C. Faurie, B. Gabriel, J. Teissie, M.P. Rols, D. Miklavcic, Effect of electric field induced transmembrane potential on spheroidal cells: theory and experiment, Eur. Biophys. J. 24 (2003) 519–528.
[33] T. Kotnik, G. Pucihar, M. Rebersek, D. Miklavcic, L.M. Mir, Role of pulse shape in cell membrane electropermeabilization, Biochim. Biophys. Acta 1614 (2003) 193–200.
[34] T. Kotnik, L.M. Mir, K. Flisar, M. Puc, D. Miklavcic, Cell membrane electropermeabilization by symmetrical bipolar rectangular pulses: Part I. Increased efficiency of permeabilization, Bioelectrochemistry 54 (2001) 83–90.
[35] M.P. Rols, J. Teissie, Electropermeabilization of mammalian cells. Quantitative analysis of the phenomenon, Biophys. J. 58 (1990) 1089–1098.
[36] E. Tekle, R.D. Astumian, P.B. Chock, Electroporation by using bipolar oscillating electric field: an improved method for DNA transfection of NIH 3T3 cells, Proc. Natl. Acad. Sci. U. S. A. 88 (1991) 4230–4234.
[37] V.A. Klenchin, S.I. Sukharev, S.M. Serov, L.V. Chernomordik, A. Chizmadzhev Yu, Electrically induced DNA uptake by cells is a fast process involving DNA electrophoresis, Biophys. J. 60 (1991) 804–811.
[38] J. Teissie, C. Blangero, Direct experimental evidence of the vectorial character of the interaction between electric pulses and cells in cell electrofusion, Biochim. Biophys. Acta 775 (1984) 446–448.
[39] G. Sersa, M. Cemazar, D. Miklavcic, Antitumor effectiveness of electrochemotherapy with *cis*-diamminedichloroplatinum(II) in mice, Cancer Res. 55 (1995) 3450–3455.
[40] D.A. Zaharoff, R.C. Barr, C.Y. Li, F. Yuan, Electromobility of plasmid DNA in tumor tissues during electric field-mediated gene delivery, Gene Ther. 9 (2002) 1286–1290.
[41] M.L. Lucas, L. Heller, D. Coppola, R. Heller, IL-12 plasmid delivery by in vivo electroporation for the successful treatment of established subcutaneous B16.F10 melanoma, Molec. Ther. 5 (2002) 668–675.
[42] C. Faurie, M. Golzio, P. Moller, J. Teissie, M.P. Rols, Cell and animal imaging of electrically mediated gene transfer, DNA Cell Biol. 22 (2003) 777–783.